

Evaluation of RPV according to alternative fracture toughness requirements

Sin-Ae Lee, Sang-Hwan Lee and Yoon-Suk Chang*

Department of Nuclear Engineering, Kyung Hee University, 1732 Deogyong-daero, Giheung, Yongin, Kyonggi, 446-701, Republic of Korea

(Received December 11, 2014, Revised February 10, 2015, Accepted February 13, 2015)

Abstract. Recently, US NRC revised fracture toughness requirements as 10CFR50.61a to reduce the conservatism of 10CFR50.61. However, unlike previous studies relating to the initial regulation, structural integrity evaluations based on the alternative regulation are not sufficient. In the present study, PTS and P-T limit curve evaluations were carried out by using both regulations and resulting data were compared. With regard to the PTS evaluation, the results obtained from the alternative requirements were satisfied with the criterion whereas those obtained from the initial requirements did not meet the criterion. Also, with regard to the P-T limit curve evaluation, operating margin by 10CFR50.61a was greater than that by 10CFR50.61.

Keywords: alternative fracture toughness requirement; PTS; P-T limit curve; radiation embrittlement

1. Introduction

RPV (Reactor Pressure Vessel) is the most important nuclear component which withstands high pressure and temperature, and harsh environments for power generation (Gonzalez-Albuixech *et al.* 2014). Relating to long-term operation, it is necessary to evaluate irradiation effects since the beltline region materials of the RPV are significantly degraded due to the fast neutron (Chou and Huang 2014, Qian and Niffenegger 2013a). Particularly, PTS (Pressurized Thermal Shock) and P-T (Pressure-Temperature) limit curve evaluations should be conducted by taking into account the irradiation embrittlement. During the operation of a NPP (Nuclear Power Plant), certain accidents could initiate the emergency cooling system for rapid cool-down of the RPV wall, so-called PTS, which may induce significant stresses in the RPV material (Chen *et al.* 2014, Qian and Niffenegger 2013b). If the stresses are high enough to initiate existing cracks in the embrittled RPV material, it may lead to crack propagation and subsequent failure of the RPV (Qian *et al.* 2014).

Meanwhile, pressure and temperature histories of the RPV should be controlled in light of P-T limit curve under normal operation, hydrostatic pressure and leak test conditions (Ren *et al.* 2013). The P-T limit curve defines the limit of the maximum pressure and minimum temperature of the connected major components in a NPP to prevent brittle fracture during the aforementioned typical transients. In case of the PWR (Pressurized Water Reactor), the procedure of generating P-T limit

*Corresponding author, Professor, E-mail: yschang@khu.ac.kr

curve was suggested in ASME (American Society of Mechanical Engineering) Code Sec. XI, App. G (ASME 2007). However, it has been known that this procedure is quite conservative so as to enhance the determination of RT_{NDT} (Reference Temperature for Nil Ductility Transition) in accordance with 10CFR50.61 (US NRC 1985).

In order to improve accuracy of the structural integrity evaluation and reduce the conservatism, US NRC (United States Nuclear Regulatory Commission) revised fracture toughness requirements as 10CFR50.61a (US NRC 2010). Although Dickson *et al.* (2011) have studied deterministic and probabilistic analyses according to 10CFR50.61a, there is a lack of related researches. In the present paper, the alternative and original requirements are examined and the values of ART (Adjusted RT_{NDT}) for a RPV are calculated based on the both regulations for PTS and P-T limit curve evaluations. Also, to demonstrate the validity, the results of this study are compared with reference data.

2. Review of fracture toughness requirements

2.1 Original requirements (10CFR50.61)

US NRC released 10CFR50.61 as fracture toughness requirements to evaluate PTS safety margin (US NRC 1985) and provided procedures to determine the RT_{PTS} which is evaluated at the end of life fluence of beltline materials. The requirements of 10CFR50.61 are used to define ART values and corresponding PTS screening criteria; 270°F (132°C) for plates, forgings and axial weld materials as well as 300°F (148.9°C) for circumferential weld materials, respectively. When the evaluated value of RT_{PTS} in the beltline region exceeds the PTS screening criteria, the licensees of each PWR should implement their own flux reduction program (Jhung *et al.* 2011).

The RT_{PTS} can be determined by the following Eqs. (1)-(3).

$$RT_{PTS} = RT_{NDT(U)} + \Delta RT_{NDT} + M \quad (1)$$

where $RT_{NDT(U)}$ is the mean value of unirradiated RT_{NDT} , M is the margin to consider uncertainties of $RT_{NDT(U)}$ and $\Delta RT_{NDT(U)}$ defined as

$$\Delta RT_{NDT} = (CF) f^{(0.28-0.10 \log f)} \quad (2)$$

where CF is the chemistry factor, f is the best estimation neutron fluence, in unit of 10^{19} n/cm² ($E > 1$ MeV), at the clad and base metal interface on the inside surface at the location where the material in question receives the highest fluence for the period of service. The f at the depth in the vessel is determined as follows.

$$f = f_{surf} \cdot e^{-0.24x} \quad (3)$$

where f_{surf} is the calculated value of the neutron fluence at the location of a postulated defect, and x is the depth into the vessel wall.

2.2 Alternative requirements (10CFR50.61a)

10CFR50.61a was revised in 2010 as an alternative of the original one. It includes RPV wall thickness dependent specific limits for axial welds, plates and forgings and circumferential welds

Table 1 Alternative PTS screening criteria

RT_{MAX-X}	RT_{MAX-X} limits [$^{\circ}\text{F}$]		
	$t_{\text{wall}} \leq 241.3$ mm	241.3 mm < $t_{\text{wall}} \leq 266.7$ mm	266.7 mm < $t_{\text{wall}} \leq 292.1$ mm
RT_{MAX-AW}	269	230	222
RT_{MAX-PL}	356	305	293
$RT_{MAX-AW} + RT_{MAX-PL}$	538	476	445
RT_{MAX-CW}	312	277	269
RT_{MAX-FO}	with underclad cracks	246	239
	w/o underclad cracks	356	293

as summarized in Table 1. The corresponding RT_{MAX-X} values such as RT_{MAX-AW} , RT_{MAX-PL} , RT_{MAX-FO} and RT_{MAX-CW} can be determined by using the following equations.

$$RT_{MAX-AW} = \text{MAX} \left\{ \begin{array}{l} RT_{NDT(U)-plate} + \Delta T_{30-plate} \\ RT_{NDT(U)-axialweld} + \Delta T_{30-axialweld} \end{array} \right\} \quad (4)$$

$$RT_{MAX-PL} = RT_{NDT(U)-plate} + \Delta T_{30-plate} \quad (5)$$

$$RT_{MAX-FO} = RT_{NDT(U)-forging} + \Delta T_{30-forging} \quad (6)$$

$$RT_{MAX-CW} = \text{MAX} \left\{ \begin{array}{l} RT_{NDT(U)-plate} + \Delta T_{30-plate} \\ RT_{NDT(U)-forging} + \Delta T_{30-forging} \\ RT_{NDT(U)-circweld} + \Delta T_{30-circweld} \end{array} \right\} \quad (7)$$

where the ΔT_{30} value can be determined by Eqs. (8)-(10).

$$\Delta T_{30} = MD + CRP \quad (8)$$

$$MD = A \times (1 - 0.001718 \times T_C) \times (1 + 6.13 \times P \times Mn^{2.471}) \times \phi_e^{0.5} \quad (9)$$

$$CRP = B \times (1 + 3.77 \times Ni^{1.191}) \times f(Cu_e, P) \times g(Cu_e, Ni, \phi_e) \quad (10)$$

where MD is the matrix damage term of the embrittlement RPV, CRP is the copper rich precipitate term of the embrittlement RPV, A and B are the constant values for each part and T_C is the reactor cold-leg temperature under normal operating full power condition. P , Mn , Ni are the estimated values for each chemical element and ϕ_e is the fast neutron fluence at each part (US NRC 2010).

The explicit margin terms in 10CFR50.61 were not taken into account for calculation of RT_{MAX-X} such as RT_{MAX-CW} . However, with regard to 10CFR50.61a, different margin terms were included in the RT_{MAX-X} limit as alternative criteria to consider uncertainties in both PTS evaluation and P-T limit curve construction (Dickson *et al.* 2011). In this study, based on the two regulations, ART values were calculated for the PTS evaluations and resulting RT_{MAX-CW} values were used for P-T limit curve evaluations of an operating RPV made of SA508 Gr.3 Cl.1 carbon steel. Hereafter, the evaluated PWR is marked as K plant for data security and convenience' sake.

Table 2 Geometry of RPV used in the present study

Parameter	Value
Inner radius of shell [mm]	1676.4
Wall thickness [mm]	165.1
Clad thickness [mm]	3.175

Table 3 Chemical parameters used in the present study

Parameter	Value
$RT_{NDT(U)}$ [$^{\circ}F$]	-10.0
Cu [%]	0.29
Ni [%]	0.68
Mn [%]	1.52
Chemistry factor [$^{\circ}F$]	190.96

Table 4 Neutron fluence according to EFPY

EFPY	Fluence [$\times 10^{19}$ n/cm ²]
24	4.25
32	5.6
40	7.04
48	8.44
60	10.6

3. PTS evaluations

3.1 Evaluation conditions

The beltline region of the RPV, which has been exposed by fast neutrons, was considered for the PTS evaluations. Since there was no axial weld in the RPV of K plant, the circumferential weld was taken into account as the critical location. The geometry and chemical data used in the present study are represented in Tables 2 and 3 (Jhung *et al.* 2011, Lee *et al.* 2013). The evaluations were carried out under 24, 32, 40, 48 and 60EFPY (Effective Full Power Years). Operating conditions and the corresponding neutron fluence data were summarized in Table 4 based on a previous study (Jhung *et al.* 1997).

3.2 Evaluation methods

To examine influences of the initial and alternative regulations, a set of PTS evaluations were performed for the aforementioned circumferential weld. Fig. 1(a) shows the procedure according to 10CFR50.61, in which the remarked box indicates changing part in 10CFR50.61a. The RT_{PTS} is calculated from initial value of RT_{NDT} for the beltline region with the margin for uncertainties of initial RT_{NDT} and ΔRT_{NDT} . Fig. 1(b) depicts the procedure according to the alternative requirement.

With regard to the PTS evaluation, it was known that the most dominant factors for RT_{MAX-X} are the neutron fluence and the chemical compositions of the RPV material. The requirements define ART values and corresponding PTS screening criteria, for which deterministic and subsequent

1275

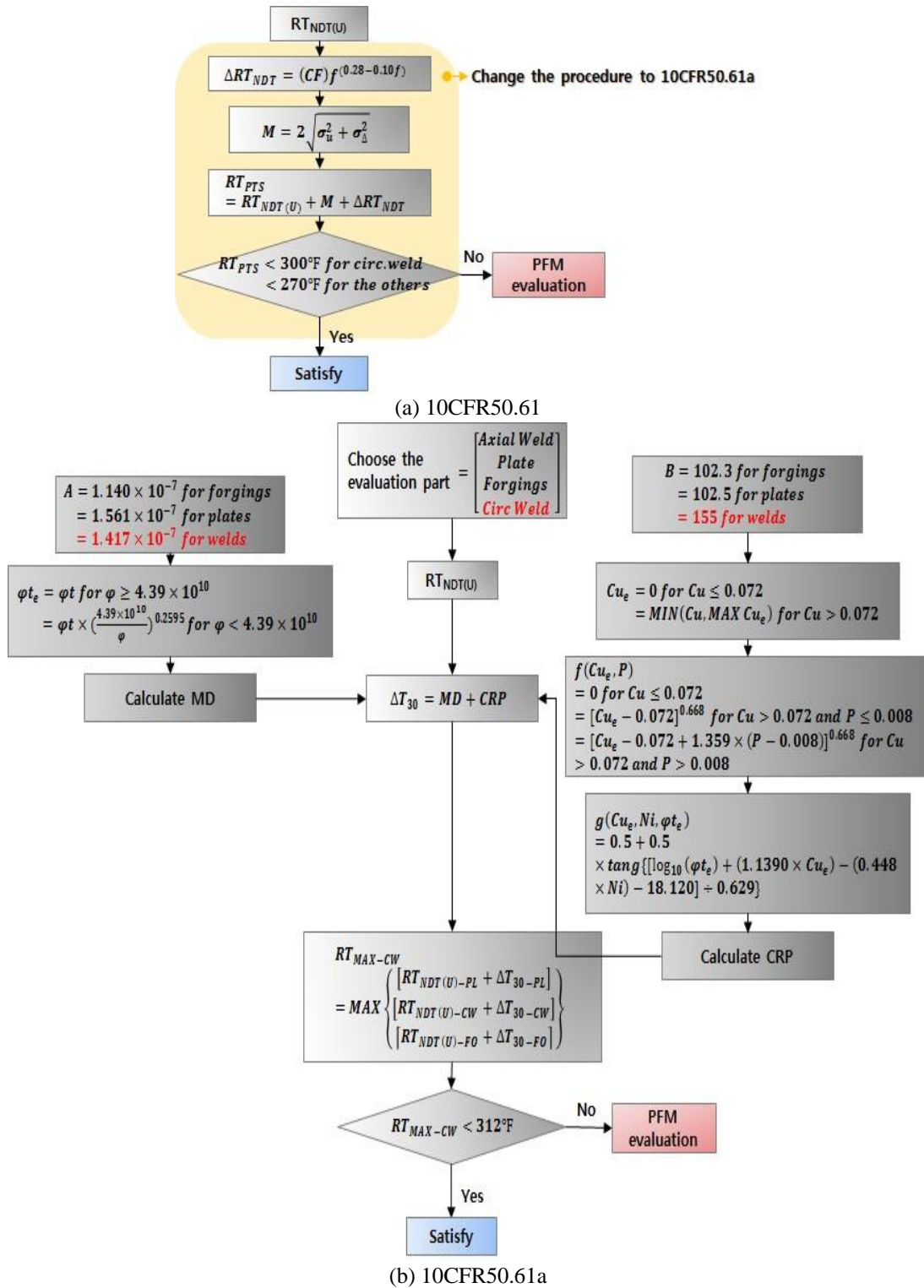


Fig. 1 Procedures used for PTS evaluation

probabilistic fracture mechanics have been employed (Qian and Niffenegger 2014). If the PTS evaluation results can not satisfy the relevant criteria, failure probability of the RPV should be quantified through the PFM (Probabilistic Fracture Mechanics) analyses (Huang *et al.* 2012). However, the PFM analysis according to 10CFR50.61a was not performed in this study, because the PTS screening criteria were satisfied as described in the following section.

3.3 Results and discussions

Fig. 2 represents two screening criteria and PTS evaluation results such as RT_{PTS} and RT_{MAX-CW} values obtained from the regulations. As shown in the figure, not only the screening criteria

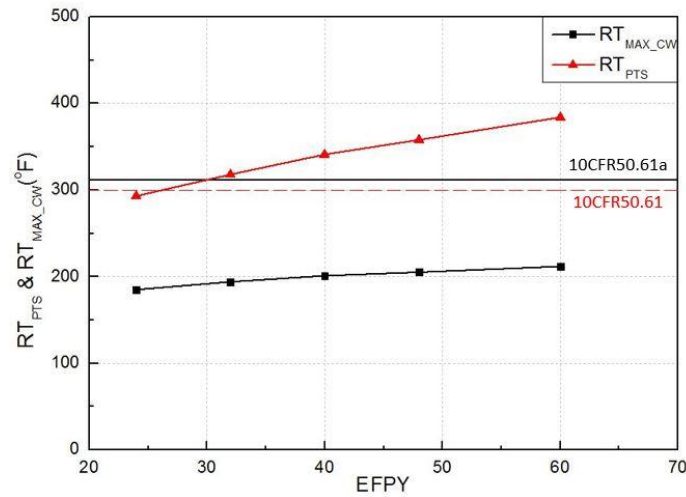


Fig. 2 PTS evaluation results

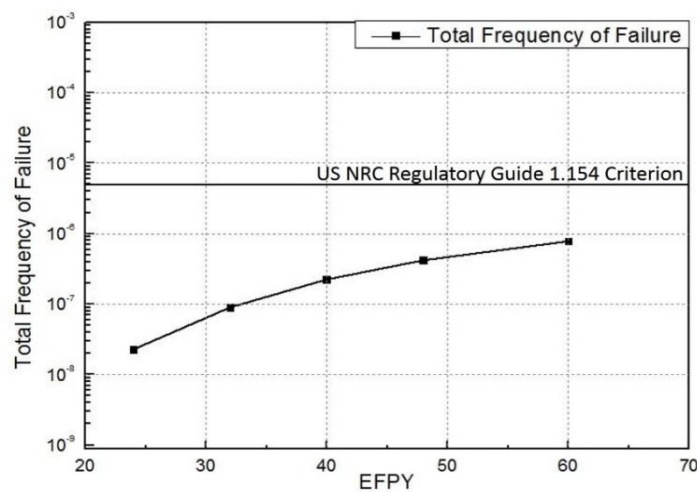


Fig. 3 PFM evaluation results

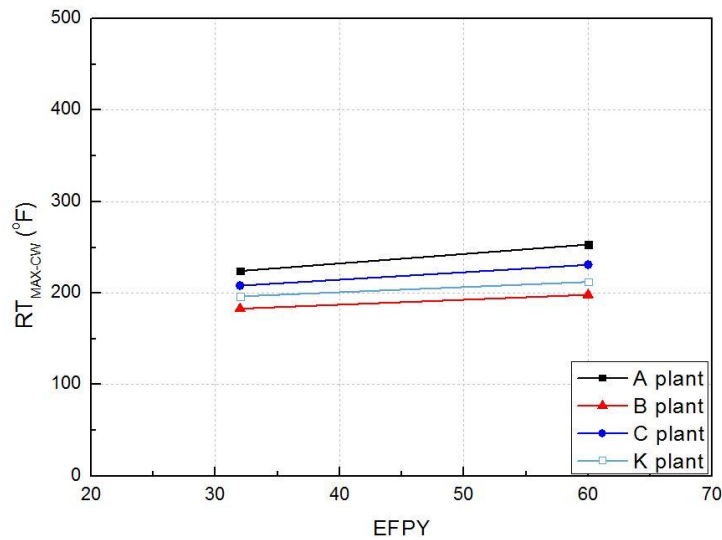


Fig. 4 Comparison of PTS evaluation results according to 10CFR50.61a

increased but also PTS evaluation results decreased when 10CFR50.61a requirements were adopted in lieu of 10CFR50.61 ones. In detail, the differences of ART ranged from 37% to 45% approximately. Also, the calculated RT_{MAX-CW} had a sufficient margin comparing to the screening criteria of 312°F (155.6°C) for circumferential weld whereas the calculated RT_{PTS} exceeded the screening criteria of 300°F (148.9°C) for the same weld at 27.5EPFY. It demonstrates that the initial regulation has significant conservatism.

Since the PTS evaluation results could not satisfy the screening criteria at 27.5EPFY, subsequent PFM evaluations were carried out in accordance with US NRC Regulatory Guide 1.154 (1987). R-PIE software (KINS 2008) was used and eight representative transients were selected based on a previous study (Jhung *et al.* 2011). The synthetic PFM evaluation results were depicted in Fig. 3, while detailed descriptions were omitted for brevity, because they were only related to the 10CFR50.61 and further enormous information should be explained. As shown in the figure, all the calculated total frequencies of failure met the acceptance criterion of $5 \times 10^{-6}/\text{yr}$. It means that the PTS issue was resolved but a great deal of effort was put into the PFM evaluations.

In order to demonstrate validity of this study, PTS evaluation data obtained from the K plant were compared with those obtained from reference NPPs in USA (Dickson *et al.* 2011) as shown in Fig. 4. All of the reference plants are the PWR like the K plant; A plant is a W/H type NPP, B and C plants are the oldest B&W and oldest CE type NPPs, respectively. The critical locations of A and B plants were circumferential welds, and in the case of plant C having critical axial weld, the difference of RT_{MAX-X} values between circumferential and axial welds was not significant. Since our concern is to examine K plant without any axial weld, the circumferential welds were compared in this study. In order to compare with the reference data, an additional PTS evaluation at 60EPFY was carried out in the present study. As shown in the figure, the highest RT_{MAX-CW} value was calculated in A plant, the lowest one was calculated in B plant and K plant was the third of them. Since the reactor materials and design types are different for each plant, the evaluated RT_{MAX-CW} values were not the same but the results derived from this study seemed reasonable because the increased tendencies of the RT_{MAX-CW} values were consistent.

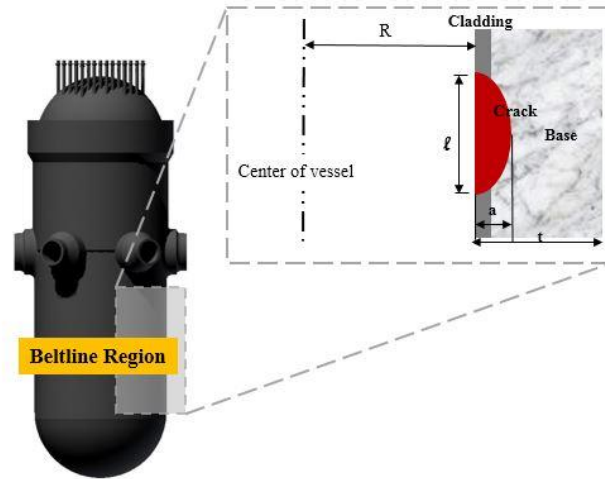
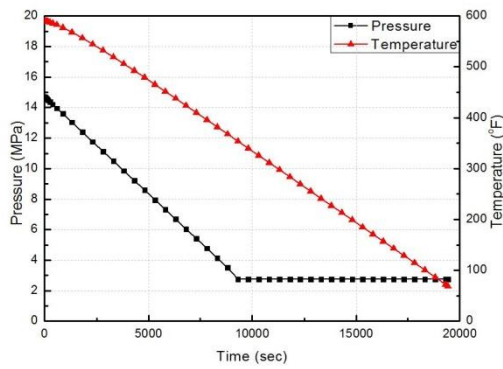
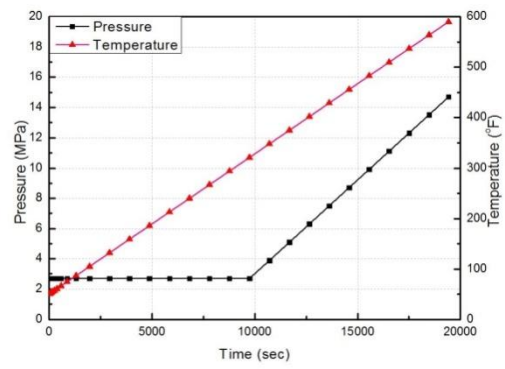


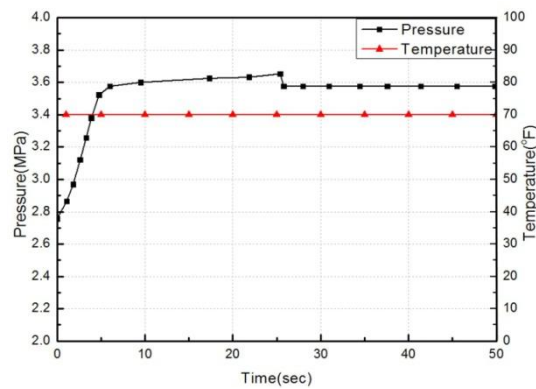
Fig. 5 A postulated semi-elliptical surface crack in the beltline region



(a) Cool-down



(b) Heat-up



(c) LTOP

Fig. 6 Pressure and temperature histories

4. P-T limit curve evaluations

4.1 Evaluation conditions

P-T limit curve evaluations were performed for a circumferential crack in circumferential weld as well as an axial crack in forging region taking into account three cool-down, heat-up and LTOP conditions because those are typical and important than hydrostatic pressure and leak test conditions. P-T limit curves were generated from the same geometry information used in the PTS evaluation. As additional information, operational pressure is 14.7MPa, operational temperature is 590°F (310°C) and shut down temperature is 69°F (20°C). The postulated defect was a surface crack with an aspect ratio (a/l) of 1/6 and a depth ratio (a/t) of 1/4 as shown in Fig. 5. With regard to the cool-down conditions, analyses were performed by considering inner surface crack because tensile stress occurred depending on the coolant temperature inside of the RPV. On the other hand, with regard to the heat-up conditions, analyses were carried out by considering outer surface crack because the tensile stress prevailed at outside of the RPV. Moreover, in case of the LTOP conditions, analyses were performed by considering both inner and outer surface cracks. The cool-down and heat-up rates were conservatively assumed as 100°F/hr (55.6°C/hr). With regard to the LTOP condition, pressure and temperature histories were quoted from a reference (Song and Yoo 2009) in which the temperature sustained constant value of 70°F (21.1°C). Fig. 6 represents pressure and temperature histories for the cool-down, heat-up and LTOP conditions. The ARTs were calculated according to both 10CFR50.61 and 10CFR50.61a at the end of the design life.

4.2 Evaluation method

ASME Code Sec. XI, App. G (2007) describes a methodology for P-T limit curve for safe operation of RPV considering the combination of thermal and mechanical stresses during the cool-down transient associated with reactor shutdown and heat-up transient associated with reactor startup (ASME 2007). The fracture criterion was developed based on LEFM (Linear Elastic Fracture Mechanics), and fracture toughness was decided from the lower bound value of testing results (Lee *et al.* 2002). Also, it provides the following equations that are used to derive the P-T limit curve for a RPV.

$$2K_{Im} + K_{It} < K_{Ic} \quad (11)$$

$$K_{Im} = M_m \left(p \frac{R_i}{t} \right) \quad (12)$$

$$K_{It_cooldown} = 0.579 \times 10^{-6} \times CR \times t^{2.5} \quad (13)$$

$$K_{It_Heatup} = 0.458 \times 10^{-6} \times HR \times t^{2.5} \quad (14)$$

where, K_{Im} and K_{It} are the time-dependent applied SIF (Stress Intensity Factor) values produced by internal pressure and thermal loading, respectively, corresponding to the specific vessel geometry and changing rate of coolant temperature. K_{Ic} is the fracture toughness, M_m is the internal pressure correction factor, p is the internal pressure, R_i is the inner radius, t is the wall thickness, CR is the cooling rate and HR is the heating rate. Eqs. (12)-(14) are only applicable for a postulated crack of $a/t=1/4$ and $a/l=1/6$ (Dickson *et al.* 2010, 2011), and the allowable pressure (P) that satisfies Eq.

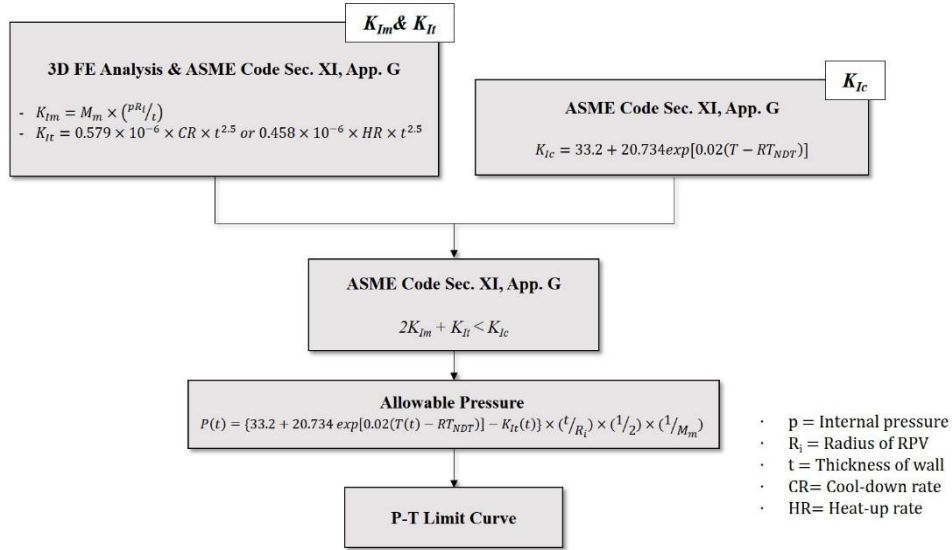


Fig. 7 Procedure used for P-T limit curve evaluation

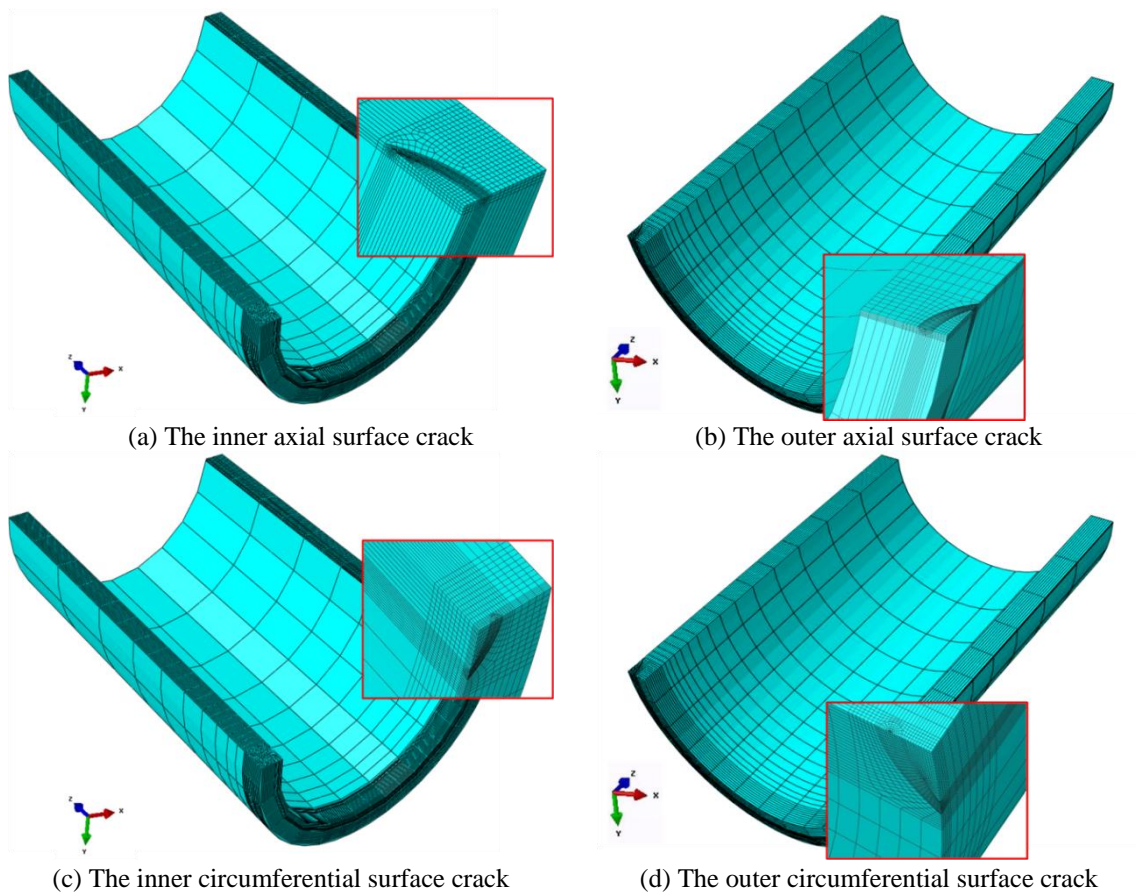


Fig. 8 FE models of RPV

(11) is obtained from the following equation.

$$P < \frac{K_{Ic} - K_{It}}{2M_m} \left(\frac{t}{R_i} \right) \quad (15)$$

A set of P-T limit curve evaluations were performed for the K plant in use of the procedure shown in Fig. 7. As mentioned before, K_{Im} and K_{It} are functions of the internal pressure and thermal loading. By comparing these K values with the fracture toughness value, the region of safety operation is defined as a function of the allowable pressures and indicated temperatures depending on time. In this study, mainly, the SIFs were calculated from three-dimensional FE (Finite Element) analyses by using a general-purpose program ABAQUS (ABAQUS version 6.13 2013). As shown in Fig. 8, the 1/4 FE models were developed by considering symmetrical features in flaw shape, geometry, material and loading condition; Figs. 8(a) and 8(b) depict the FE models of beltline region with the inner or outer axial surface crack and Figs. 8(c) and 8(d) represent those with the circumferential inner or outer surface crack of RPV. These models were generated by 20-node quadrilateral element types (DC3D20 for heat transfer analysis and C3D20R for the stress analysis in ABAQUS library). The number of elements ranged from 9,864 to 11,924 and number of nodes ranged from 45,753 to 52,861 according to the crack location. Internal pressure was applied to perpendicular direction to inside of the RPV with the end-cap force at the end of the model. The mechanical and thermal SIFs were calculated at the deepest point of semi-elliptical surface crack from FE analyses.

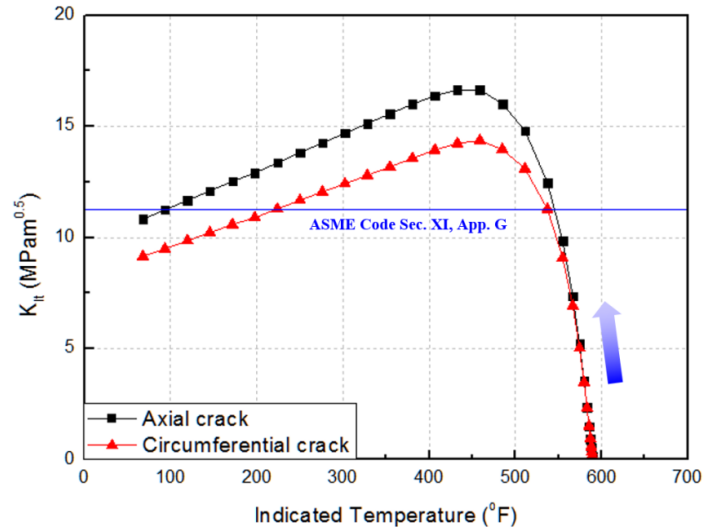
4.3 Results and discussions

Table 5 represents the comparison of maximum K_{It} values obtained from FE analyses, and ASME code based Eqs. (13) and (14) except for the LTOP conditions without corresponding equation. Generally, the K_{It} values of the axial crack in forging area were approximately 12.5% higher than those of the circumferential crack in circumferential weld due to the different crack orientations. Also, with regard to the cool-down and heat-up conditions, the K_{It} values from ASME code equations were much lower than those from FE analyses due to the crack face effect, which observation was similar with a previous research (Lee *et al.* 2002).

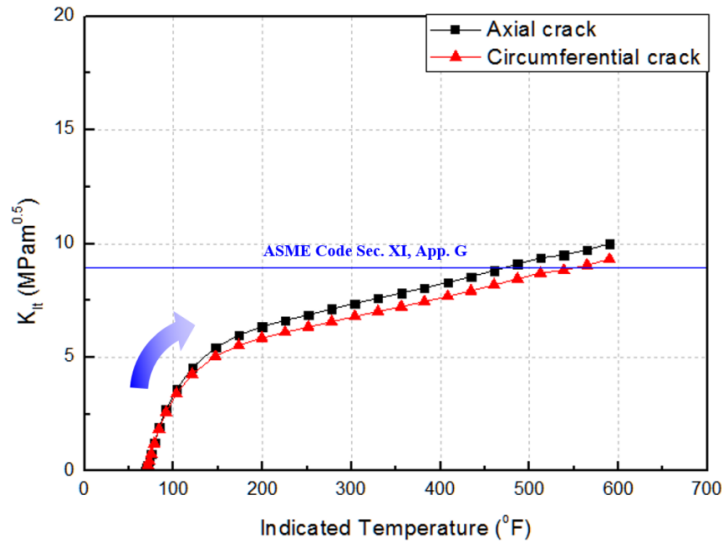
Fig. 9 shows FE calculated K_{It} variations depending on temperatures under the cool-down and heat-up conditions. With regard to the LTOP conditions, the K_{It} variation was not illustrated because the values were independent on temperatures. In the cool-down and heat-up conditions, the constant maximum K_{It} values calculated by Eqs. (13) and (14) were also represented. The values of K_{It} under cool-down conditions were increased up to around 458°F (236°C) and then decreased whereas the values of K_{It} under heat-up conditions continuously increased up to 590°F

Table 5 Comparison of maximum K_{It} values

Crack orientation	Condition	K_{It} [MPa \sqrt{m}]		
		FE analysis	ASME code	Difference
Axial crack for forging	Cool-down	16.65	11.28	32%
	Heat-up	9.99	8.91	11%
Circumferential crack for circumferential weld	Cool-down	14.37	11.28	21%
	Heat-up	9.31	8.91	4.3%



(a) Cool-down condition

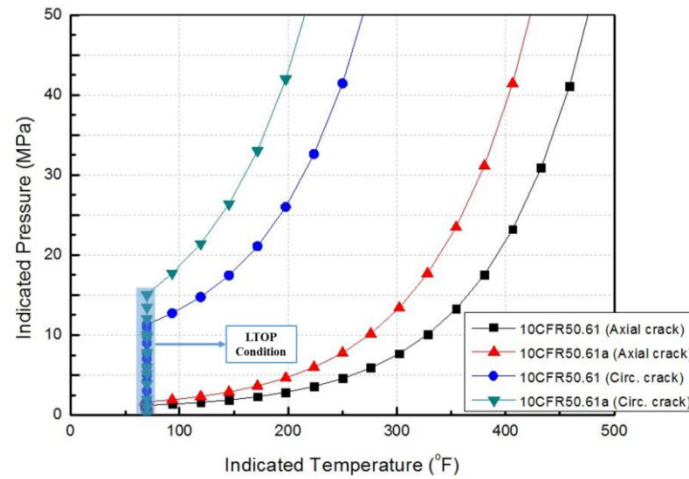


(b) Heat-up condition

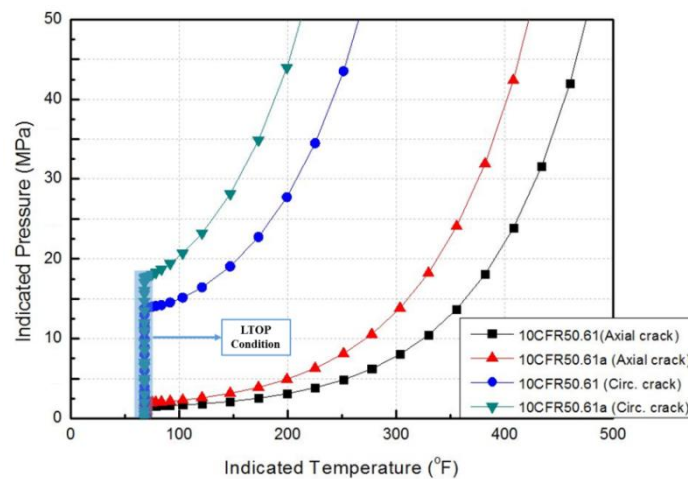
Fig. 9 K_{It} obtained from FE analyses

(310°C). In addition, as to the cool-down conditions, K_{It} values between axial and circumferential cracks were almost same in the temperature range from 590°F (310°C) to 560°F (293.3°C). On the other hand, under the heat-up conditions, K_{It} values were the same up to around 100°F (37.8°C) and then the values differed from the next.

The P-T limit curves for 10CFR50.61 and 10CFR50.61a under the cool-down and LTOP conditions were generated as shown in Fig. 10(a). Also, Fig. 10(b) represents P-T limit curves for both regulations under the heat-up and LTOP conditions. With regard to the LTOP conditions, as described previously, the allowable pressure did not change regardless of indicated temperatures because the analyses were performed under the constant temperature of 69°F (20°C). As shown in



(a) Cool-down and LTOP conditions



(b) Heat-up and LTOP conditions

Fig. 10 P-T limit curve evaluation results

the figures, the operating areas of circumferential crack were about twice larger than those of axial crack, which means the axial crack led to relatively conservative results. In case of the axial crack under cool-down and LTOP conditions, the temperatures corresponding to the operating pressure of 14.7MPa were 311.7°F (155°C) in the alternative regulation and 368°F (186°C) in the initial regulation, respectively. The difference of temperatures was approximately 56.3°F (13.5°C). Moreover, with regard to the axial crack under heat-up and LTOP conditions, the temperatures corresponding to the operating pressure were 300.75°F (149°C) in the alternative regulation and 350.75°F (176°C) in the original regulation, respectively. The difference of temperatures was approximately 50°F (10°C). This means that the operating margin based on 10CFR50.61a became also larger than the result based on 10CFR50.61.

In order to demonstrate validity of this study, the P-T limit curve of K plant was compared with those obtained from reference data (Jang 2002, Lee *et al.* 2002, Park *et al.* 2010) as shown in Fig.

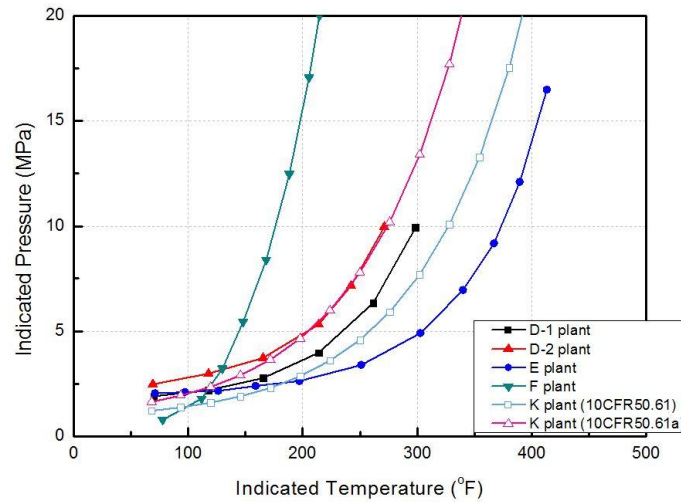


Fig. 11 Comparison of P-T limit curve evaluation results for the axial crack under cool-down condition

11. All of P-T limit curves were generated according to 10CFR50.61 requirements due to lack of detailed data based on the alternative regulation. The referenced P-T limit curves were delineated as D-1, D-2, E and F plants by considering different analysis conditions and reactors. As shown in the figure, the highest operating margin was obtained from F plant while the lowest one was obtained from E plant. The P-T limit curve of D-2 plant was quite similar to that of K plant due to the comparable conditions. Since the reactor materials and design types are different for each plant, the evaluated P-T limit curves were not the same but the results derived from this study seemed reasonable because the increased tendencies of the allowable pressures were consistent according to the indicated temperatures. Despite brief comparison of P-T limit curves was performed in the present study, detailed assessment may be available if specific information is gathered in the future.

5. Conclusions

In the present study, two kinds of structural integrity evaluations were carried out for a typical RPV by using alternative regulation (10CFR50.61a) as well as initial regulation (10CFR50.61). Thereby, the following key findings have been derived.

- As a result of PTS evaluation, calculated RT_{PTS} values according to the initial regulation exceeded the screening criteria of 300°F (148.9°C) for circumferential welds at 27.5EFPY. However, RT_{MAX-CW} values according to the alternative regulation had sufficient margin about the screening criteria of 312°F (155.6°C) for the same welds.

- As a result of P-T limit curve evaluation, it was proven that the operating margin from 10CFR50.61a is larger than the initial regulation. Quantitatively, in case of the axial crack, temperatures corresponding to the operating pressure of 14.7MPa obtained from the both regulations had differences of 50°F (10°C)~56.3°F (13.5°C) while effects of the cool-down, heat-up and LTOP conditions were not significant. In addition, the operating areas of circumferential crack were about twice larger than those of axial crack.

• In order to demonstrate validity, results of this study compared with limited reference data. With regard to the PTS evaluations, the present results seemed reasonable because the linearly increasing tendencies of the RT_{MAX-CW} values were consistent according to EPFY. Also, with regard to the P-T limit curve evaluations, the present results were still reasonable because the varying tendencies of the allowable pressure were similar according to the indicated temperatures while they were not perfectly consistent due to parabolic characteristics.

References

- ABAQUS version 6.13 (2013), ABAQUS Standard/User's Manual, Simulia Inc.
- ASME (2007), Boiler and Pressure Vessel Code, Section XI, Fracture Toughness Criteria for Protection against Failure, Appendix G.
- Chen, M., Lu, F., Wang, R. and Ren, A. (2014), "Structural integrity assessment of the reactor pressure vessel under the pressurized thermal shock loading", *Nucl. Eng. Des.*, **272**, 84-91.
- Chou, H.W. and Huang, C.C. (2014), "Effects of fracture toughness curves of ASME section XI- Appendix G on a reactor pressure vessel under pressure-temperature limit operation", *Nucl. Eng. Des.*, **280**, 404-412.
- Dickson, T.L., Fochr, E. and Kirk, M. (2010), "Review of proposed methodology for a risk-informed relaxation to ASME Section XI - Appendix G", *Proceedings of ASME 2010 Pressure Vessels & Piping Division Conference*, PVP2010-25010 in CD-ROM, Bellevue, Washington, USA.
- Dickson, T.L., Yin, S.J., Kirk, M. and Chou, H.W. (2011), "Derivation of the new pressurized thermal shock screening criteria", *Proceedings of ASME 2011 Pressure Vessels & Piping Division Conference*, PVP2011-57008 in CD-ROM, Baltimore, Maryland, USA.
- Gonzalez-Albuixech, V.F., Qian, G. and Niffenegger, M. (2014), "Integrity analysis of reactor pressure vessels subjected to pressurized thermal shocks by XFEM", *Nucl. Eng. Des.*, **275**, 336-343.
- Huang, C.C., Chou, H.W., Chen, B.Y., Liu, R.F. and Lin, H.C. (2012), "Probabilistic fracture analysis for boiling water reactor pressure vessels subjected to low temperature over-pressure event", *Annal. Nucl. Energy*, **43**, 61-67.
- Jang, C.H. (2002), "Construction of the P-T limit curve for the nuclear reactor pressure vessel using influence coefficient methods: cooldown curve", *J. Mech. Sci. Tech.*, **26**(3), 505-513.
- Jhung, M.J., Choi, Y.H. and Chang, Y.S. (2011), "Comparison of vessel failure probabilities during PTS for Korean nuclear power plants", *Struct. Eng. Mech.*, **37**(3), 257-265.
- Jhung, M.J., Park, Y.W. and Lee, J.B. (1997), "Integrity evaluation of Kori 1 reactor vessel for Rancho Seco transient", *J. KSME*, **21**(7), 1089-1096.
- KINS (2008), Reactor Probabilistic Integrity Evaluation (R-PIE) Code: User's Guide, Korea Institute of Nuclear Safety, Daejeon.
- Lee, T.J., Choi, J.B., Kim, Y.J. and Park, Y.W. (2002), "A parametric study on pressure-temperature limit curve using 3D finite element analyses", *Nucl. Eng. Des.*, **214**, 73-81.
- Park, S.Y., Kim, J.Y. and Kim, T.W. (2010), "Evaluation of P-T limit curve for reactor pressure vessel using finite element analysis", *The KSME Fall Annual Conference*, Jeju, Korea.
- Qian, G. and Niffenegger, M. (2013a), "Integrity analysis of a reactor pressure vessel subjected to pressurized thermal shocks by considering constraint effect", *Eng. Fract. Mech.*, **112-113**, 14-25.
- Qian, G. and Niffenegger, M. (2013b), "Procedures, methods and computer codes for the probabilistic assessment of reactor pressure vessels subjected to pressurized thermal shocks", *Nucl. Eng. Des.*, **258**, 35-50.
- Qian, G., Gonzalez-Albuixech, V.F. and Niffenegger, M. (2014), "Probabilistic assessment of a reactor pressure vessel subjected to pressurized thermal shocks by using crack distributions", *Nucl. Eng. Des.*, **270**, 312-324.
- Qian, G. and Niffenegger, M. (2014), "Deterministic and probabilistic analysis of a reactor pressure vessel

- subjected to pressurized thermal shocks”, *Nucl. Eng. Des.*, **273**, 381-395.
- Ren, A., Lu, F., Chen, M. and Wu, H. (2013), “Influence of temperature related parameters on P-T limit curves for RPV”, *J. Mech. Strength*, **35**(4), 454-459.
- Song, D.S. and Yoo, S.S. (2009), “LTOP evaluation for continued operation for NPP”, *The KSME Fall Annual Conference*, Pyeongchang, Gangwon, Korea.
- US NRC (1985), Fracture Toughness Requirements for Protection against Pressurized Thermal Shock Events, 10CFR50.61, US Nuclear Regulatory Commission, Washington, DC.
- US NRC (1987), Format and Content of Plant-specific Pressurized Thermal Shock Analysis Reports for Pressurized Water Reactor, Regulatory Guide 1.154, US Nuclear Regulatory Commission, Washington, DC.
- US NRC (1988), Radiation Embrittlement of Reactor Vessel Materials, Regulatory Guide 1.99, Rev.2, US Nuclear Regulatory Commission, Washington, DC.
- US NRC (2010), Alternative Fracture Toughness Requirements for Protection against Pressurized Thermal Shock Events, 10CFR50.61a, US Nuclear Regulatory Commission, Washington, DC.

CC

Nomenclature

A	: Constant values of matrix damage term for each part
B	: Constant values of copper rich precipitate term for each part
CF	: Chemistry factor
CRP	: Copper rich precipitate term
f	: Neutron fluence in the vessel wall
f_{surf}	: Calculated value of the neutron fluence
K_{Ic}	: Fracture toughness
K_{Im}	: Stress intensity factor by internal pressure
K_{It}	: Stress intensity factor by thermal stress
M	: Margin which considers the uncertainties of $RT_{NDT(U)}$ and $\Delta RT_{NDT(U)}$
M_m	: Internal pressure correction factor
MD	: Matrix damage term
Mn	: Manganese content
Ni	: Nickel content
p	: Internal pressure
P	: Phosphorus content
RT_{MAX-AW}	: Resistance of RPV to fracture initiating from flaws at axial weld
RT_{MAX-CW}	: Resistance of RPV to fracture initiating from flaws at circumferential weld
RT_{MAX-FO}	: Resistance of RPV to fracture initiating from flaws at forging
RT_{MAX-PL}	: Resistance of RPV to fracture initiating from flaws at plate
RT_{NDT}	: Reference temperature for nil ductility transition
$RT_{NDT(U)}$: Initial reference temperature for nil ductility transition
R_i	: Inner radius
T_C	: Reactor cold leg temperature under full power operating conditions
t	: Wall thickness
x	: Depth of vessel
ϕt_e	: Fast neutron fluence for neutron with energetic greater than 1.0MeV